STUDIES ON GENERATION AND TRANSPORT OF SODIUM AEROSOLS IN SOME TEST FACILITIES

T. SANO and T. SHIMOMURA

Mitsubishi Heavy Industries, Ltd.,
Tokyo, Japan

N. HATTORI

Power Reactor and Nuclear Fuel
Development Corporation
Tokyo, Japan

ABSTRACT

Technical experiences that have been obtained during the course of the experiments to determine the sodium aerosol concentration, to study the deposition of sodium aerosol, and to predict mechanical properties of sodium vapor deposits are presented.

In the first study, the sodium aerosol concentrations in an inert cover gas space over a sodium pool and those following a sodium spray injection into an inert atmosphere were determined. The results from the two different experiments were compared with each others and were discussed in comparison with those from the literature.

In the second study, deposition of sodium aerosol following a sodium spray injection into an inert atmosphere was examined. The deposition rates on the walls and the floor of a closed concrete cell were measured, and the results obtained were discussed.

The third study relates to the sodium vapor deposition within a narrow annulus. In the experiments, a downward argon gas flow that passes the annulus was fed to prevent sodium vapor deposition. Average sodium vapor deposition rates on the walls of the annulus were determined, then the effect of the downward feed gas was discussed.

The last study relates to one of the mechanical properties and the deformation rate of solid sodium being compressed. The purpose of the experiments were to obtain data to predict deformation rate of the sodium deposits.

INTRODUCTION

Engineering data on the generation, transport and deposition of sodium mist or aerosols, in the closed gas space, are important factor for the design and operation of the LMFBR reactor cover gas systems.

In these fields, the main efforts have been directed toward the study on the behavior of heat and mass transfer of sodium aerosol and the method to avoid sodium vapor deposition, for the purpose of the development of components with high reliability. In addition, basic studies have been performed on the mechanical properties of the deposited or frozen sodium in order to find out what force would be required to remove solidified sodium even if sodium deposition may adhere to the structure.

In this report, the results of our recent study concerning the above-mentioned points are briefly presented.

1. DETERMINATIONS OF AEROSOL CONCENTRATION

Mass concentrations of sodium mists or aerosols generated from a pool surface and from dispersed sodium spray droplets, both in an inerted atmosphere, were determined experimentally. Then the results obtained were discussed and some of them were compared with those in the literature.

(1) Determination of Sodium Aerosol Concentration over a Sodium Pool

An experimental apparatus shown in Fig.1 was used to determine the sodium aerosol concentration over a sodium pool surface. In the experiment, argon gas was fed into the test pot through TEST SECTIONS A,B,C, or D and was blown down directly toward a pool surface at a flow rate of 10 Nl/min. The excess gas was exhausted continuously through a vapor trap. In the vapor trap, the sodium aerosol suspended in the exhausted gas was collected. Sodium aerosol concentration was determined from the weight of collected aerosol in the vapor trap and the total gas flow that passed through the vapor trap.

Figure 2 shows the results as a function of the sodium pool temperature. The saturated vapor concentrations at the present cover gas temperatures and the aerosol concentrations from reference [1] that had been obtained under the cover gas natural convective condition are also shown in the same figure. It is seen that the present concentrations are approximately one order higher than those from the reference. This is probably attributed to an enhancement of sodium evaporation due to the gas blow down during the present experiment. In the LMFBR cover gas system design, the present results should be taken into account, in particular, in the design of a vapor trap where a comparatively large gas flow rate may sometimes through.

(2) Sodium Aerosol Concentrations Following a Sodium Spray Fire Experiment

During a series of sodium spray fire experiments within an inerted atmosphere (i.e., a nitrogen atmosphere), sodium aerosol concentrations and their changes were measured. Here, its results are presented and discussed in comparison with those presented in Fig.2.

In the experiment, a sodium spray was generated from a full cone spray nozzle located at 3 m above a floor in a concrete cell having an inner volume of 21 cubic meters. The spraying time was approximately one minute. A series of spray experiments were conducted in this way. The mean droplet size in the experiments ranged from 1.5mm to 2.5mm.

Figure 3 shows the results against the time from the spray initiation. It is seen that the initial concentrations do not so differ greatly from experiment to experiment. They are insensitive to the spray droplet size. In addition, the initial (i.e. the maximum) concentrations of about 20 g/m^3 seen in Fig.3 is comparable with the sodium aerosol concentrations shown in Fig.2 at the same sodium temperature. These facts allow us to conclude that, in an inerted atmosphere, the concentration of sodium aerosol depends primarily on the sodium temperature. The concentration is insensitive to the condition of gas convection in the vicinity of the sodium surface, and the sodium surface area exposed to an inert gas.

2. DATA ON THE TRANSPORT AND DEPOSITION OF SODIUM AEROSOL

Summarized here is experimental data on the transport and deposition of aerosol after the spraying in the above-mentioned nitrogen filled tests.

Illustrated in Fig.4 is the transition with time of sodium aerosol settling flux on the floor. The flux was measured by inserting a settling sampler dish from outside at a certain interval in an air-lock method.

Fig.5 shows an example of data of the time transition of sodium deposition flux on the side wall, after spray discharge in the nitrogen-filled closed space. The settling flux is fairly greater than the deposition flux. The settling flux is large especially for the first hour or so. The sharp drop in concentration shown in Fig.3 is probably due to the settling of aerosols.

Given that Stokes' law is applicable to the settling of particles, the falling velocity Vt of particles from approx. 1 to 10 microns in size is given as follows:

$$Vt \propto d^2 \qquad \text{.....................} \quad (1)$$

where Vt: terminal falling velocity (m/h)
d : particle diameter of aerosol (m)

The in-space suspension time t_f (h) is in inverse proportion to Vt and given as follows:

$$t_f \propto \frac{1}{Vt} \propto \frac{1}{d^2} \qquad \text{.....................} \quad (2)$$

The mass m of aerosol is proportional to the cube of the particle size and therefore the settling rate W is given by the following equation:

$$W = \frac{m}{t_f} \propto d^5 \qquad \text{.....................} \quad (3)$$

If the equation can be applicable to respective particle sizes with a size distribution, the time transition for a given particle size can be derived from the time transitional measurements of the settling rate. In the present experiment, the particle size was derived as follows:

$$d \propto t^{-0.52} \qquad \text{.....................} \quad (4)$$

where t: elapsed time (h)

The transitional aerosol mass mean diameter was measured by the cascade impactor, and the results are shown in Fig.6. The results are in good agreement with the calculation from Equation (4).

The aerosol deposition flux was small compared with the settling flux because of the marked decay of the concentration. The mass transfer coefficient K of the deposition of aerosol, defined by the following equation can be obtained from the measurements of the deposition flux.

$$K = Wd/C \qquad \text{.....................} \quad (5)$$

where K : mass transfer coefficient (m/h)
Wd: aerosol deposition flux (kg/m^2h)
C : aerosol concentration (kg/m^3)

The coefficients K as obtained in experiments TASP-N3 and TASP-N5 were:

Experiment TASP-N3 ..... K = 0.05 - 0.5 (m/h)
Experiment TASP-N5 ..... K = 0.6 - 1 (m/h)

3. EFFECT OF DOWNWARD FEED GAS FLOW ON SODIUM DEPOSITION ON ANNULAR WALLS

Experiments to seek a way of preventing the upward flow of radioactive gas and sodium vapor by downward feed gas on annular walls have been reported in ref. [2].

Here the effect of downward feed gas flow on sodium deposition is described.

The test section installed in the experimental apparatus shown at the left hand side of Fig.1 was used for the experiment. The test section is about 800mm in height. It consists of an inner cylinder with an outer diameter of 80mm and an outer pipe with an inner diameter of 96mm. An annular space thus provided is 800mm in height and 2mm in gap width. The principle to prevent sodium vapor deposition is to feed a downward gas flow through the annulus. In the experiment, sodium vapor was deposited on the annular walls of the test section for a certain period of time. Then the test section was disassembled, and the sodium deposit was recovered to determine the deposition rate.

Fig.7 shows the measured average sodium deposition rate on the inner and the outer walls versus sodium pool temperature. It is seen that the average deposition rate on the inner wall is higher than that on the outer wall. This implies that cold gas blew out in a downward direction along the outer wall. Examination on the flow pattern of the downward feed gas using a transparent test section having the same geometrics indicated that the cold feed gas flowed along the outer wall. It was concluded therefore, that the difference in the deposition rates on the outer and the inner walls seen in Fig.7 was due to this flow pattern. According to the previous work [2], the condition to prevent the buoyant flow by downward feed gas is controlled by $Gr/Re^{1.43}/Fr^{0.35}$. The experimental results for sodium deposition are summarized in Fig.8. As shown in Fig.8, the conditions of the feed gas to prevent deposition on annular walls with different gaps can be given by the following equation:

$$\frac{Gr}{Re^{1.43}Fr^{0.35}} \leqq 32.5 \qquad \text{.....................} \qquad (6)$$

where Gr: Grashoff number
Re: Reynolds number
Fr: Froude number

It is noted that the temperature difference between gas in the lower area and blow gas, is taken as the temperature difference for Grashoff number. And the equivalent length is twice the gap in the annular wall.

4. BASIC DATA ON COMPRESSION FORCE TO REMOVE THE DEPOSITED AND FROZEN SODIUM

Obviously the study on the method to avoid sodium deposition is important on the basis of the design criteria to avoid sodium deposition. However, a design philosophy to permit sodium deposition can be an alternative method.

In this case, the knowledge about how to remove solidified sodium, is necessary. Therefore, we have put emphasis upon the studies concerning the mechanical strength of sodium [3]. In the latest of that series of studies, basic experiments were conducted to find out what force would be required to press out solid sodium by means of compressive force. This data is required to remove sodium deposition sticking to areas where components are engaged with each other. Fig.9 shows an example of data obtained when specified loads were applied in normal direction to solid sodium with a thickness of 20mm. Test results can be summarized as follows:

- The deformation rate of the solid sodium was comparatively fast at the initial stage of compression. Then the compression proceeded very slowly.
- The residual thickness after the initial fast deformation was smaller at a higher temperature or under a larger load. Also, the smaller the compression opening, the larger the initial residual thickness.
- Decrease in thickness after the initial compression: In case the compressive stress was not higher than 20 kg/cm^2, the residual thickness was in proportion to the time raised to - 1/4th power. If the compressive force was larger, the reduction slowed down further.

5. CONCLUSIONS

Technical experiences that have been obtained during the source of the experiments on determination of sodium aerosol concentration, to study deposition of sodium aerosol, and to predict mechanical properties of sodium vapor deposits are presented. The summaries of the results presented are as follows:

(1) Concentrations of sodium aerosol over a sodium pool, and following a sodium spray fire experiment both in an inert atmosphere were determined. The comparison of the results from these two different experiments revealed that sodium aerosol concentration depends primarily on the sodium temperature. The flow condition of gas in the vicinity of the sodium surface and the surface area of sodium are found to be a secondary controlling factors.
(2) In dispersed spray experiments in a closed space, aerosol settling flux and deposition were measured. Then aerosol settling flux, transition with time of aerosol particle size, and mass transfer coefficient for deposition on wall were discussed quantitatively.
(3) An empirical formula on the relationship between the sodium deposition on annular walls and the condition of the downward feed gas was obtained (see Eq.(6)).
(4) Basic data on the compression of solid sodium was acquired. Solid sodium can be compressed easily until it is several millimeters in thickness. After this, the compression proceeds very slowly.

REFERENCE

[1] Y. Himeno et al., IAEA IWGFR Specialist's Meeting on "Aerosol Formation, Vapor deposits and Vapor Trapping" Cadarache, France (1976).
[2] K. Yamamoto et al., Proceedings of 2nd Int. Conf. on Liquid Metal Technology in Energy Production (1980).
[3] S. Ueda et al., Proceedings of 3rd Int. Conf. on Liquid Metal Technology in Energy Production (1984).

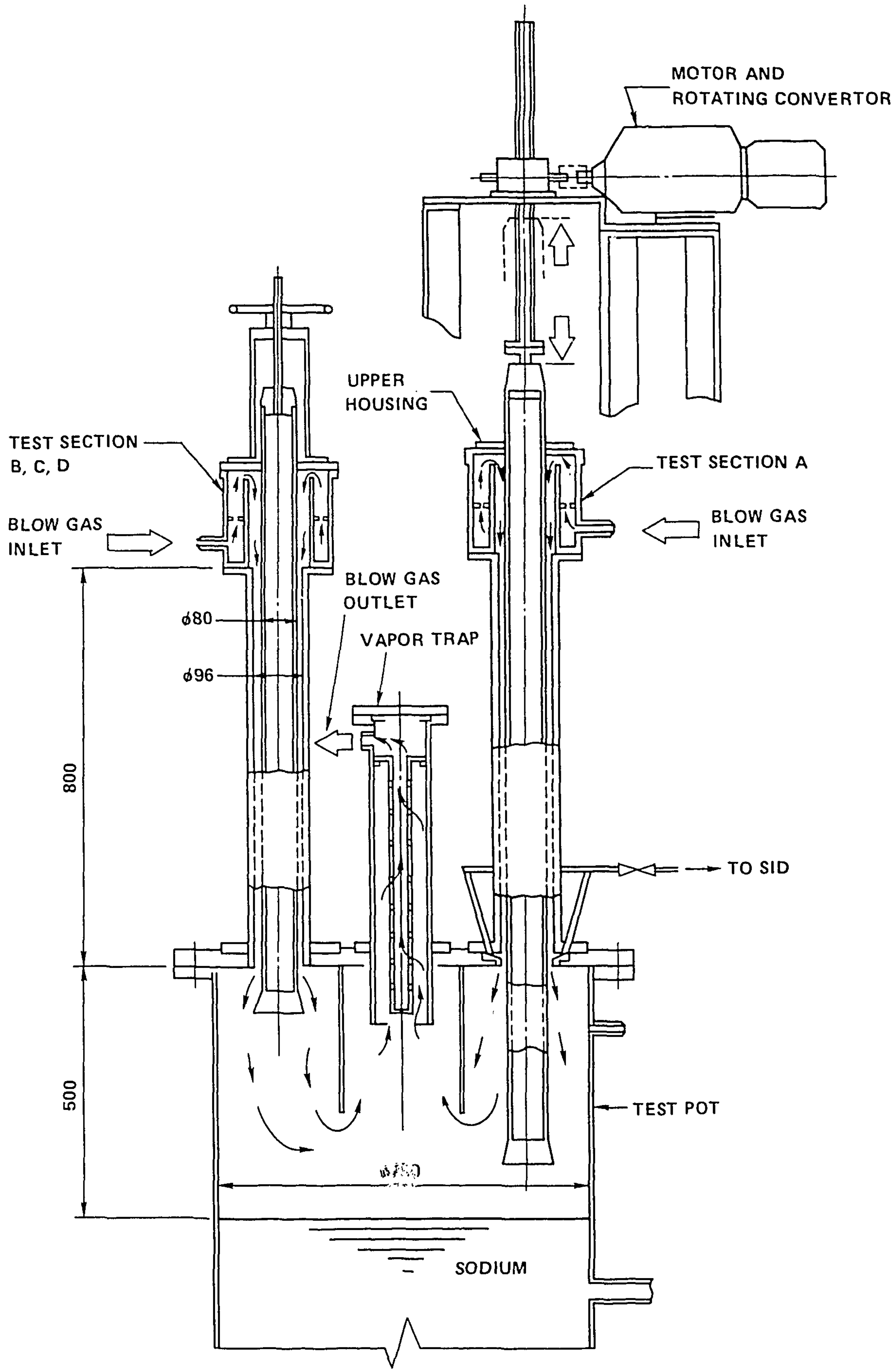

Fig. 1 Schematic Figure of Test Equipment (Vapor Deposition Test)

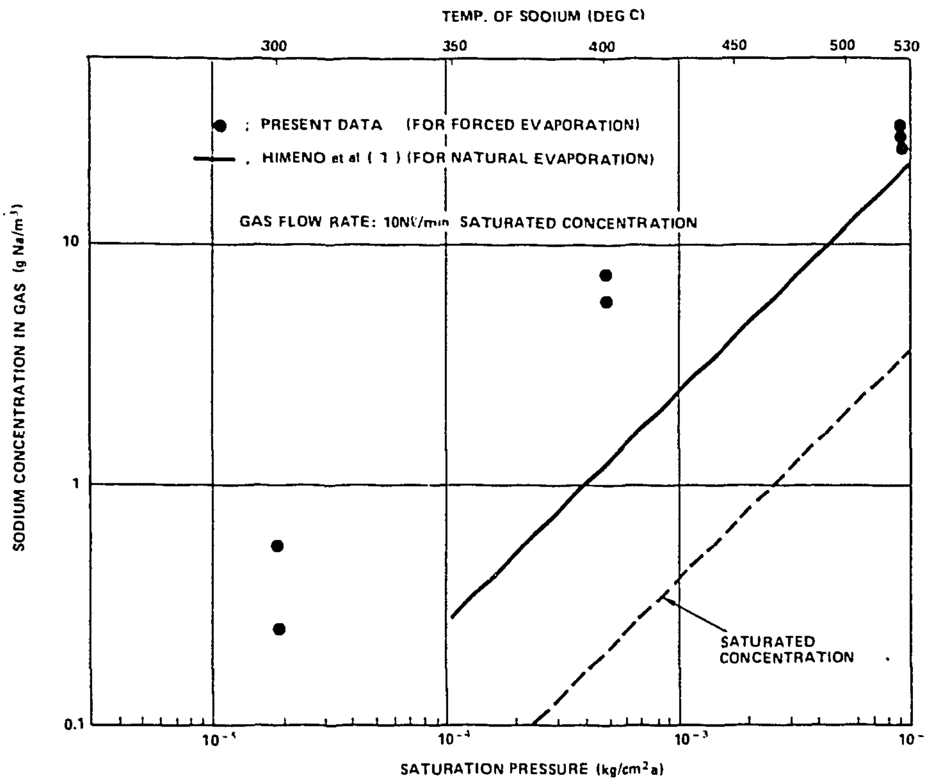

Fig. 2 Sodium Concentration in Gas in Tests with Forced Convective Gas Flow

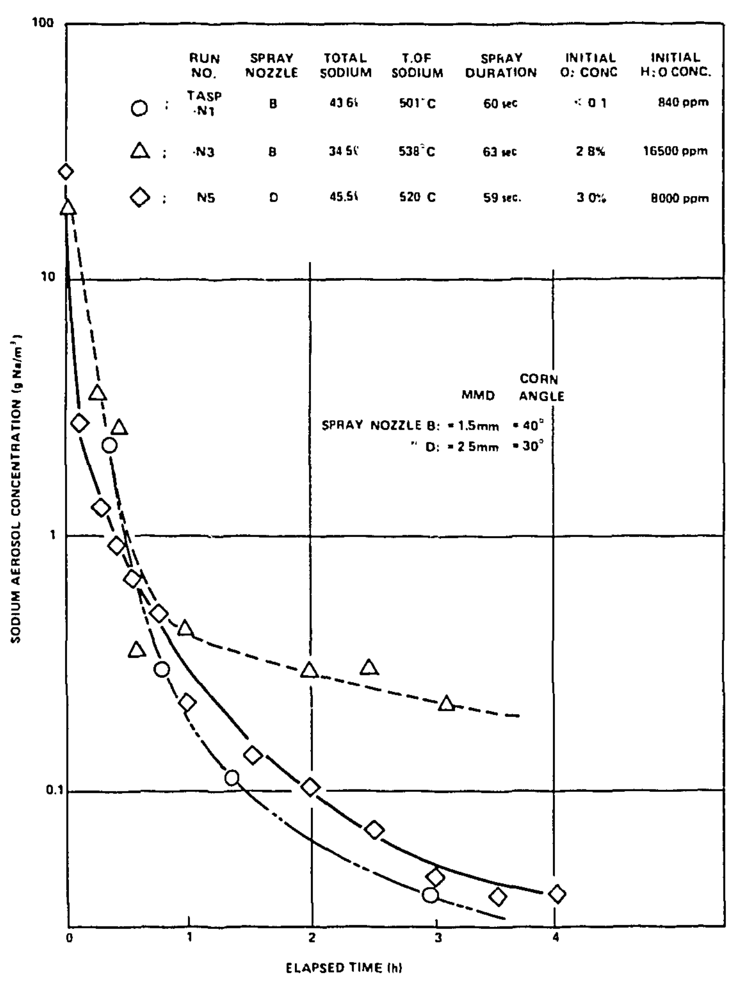

Fig. 3 Sodium Aerosol Concentration after Spray Discharge in Nitrogen-filled Closed Space

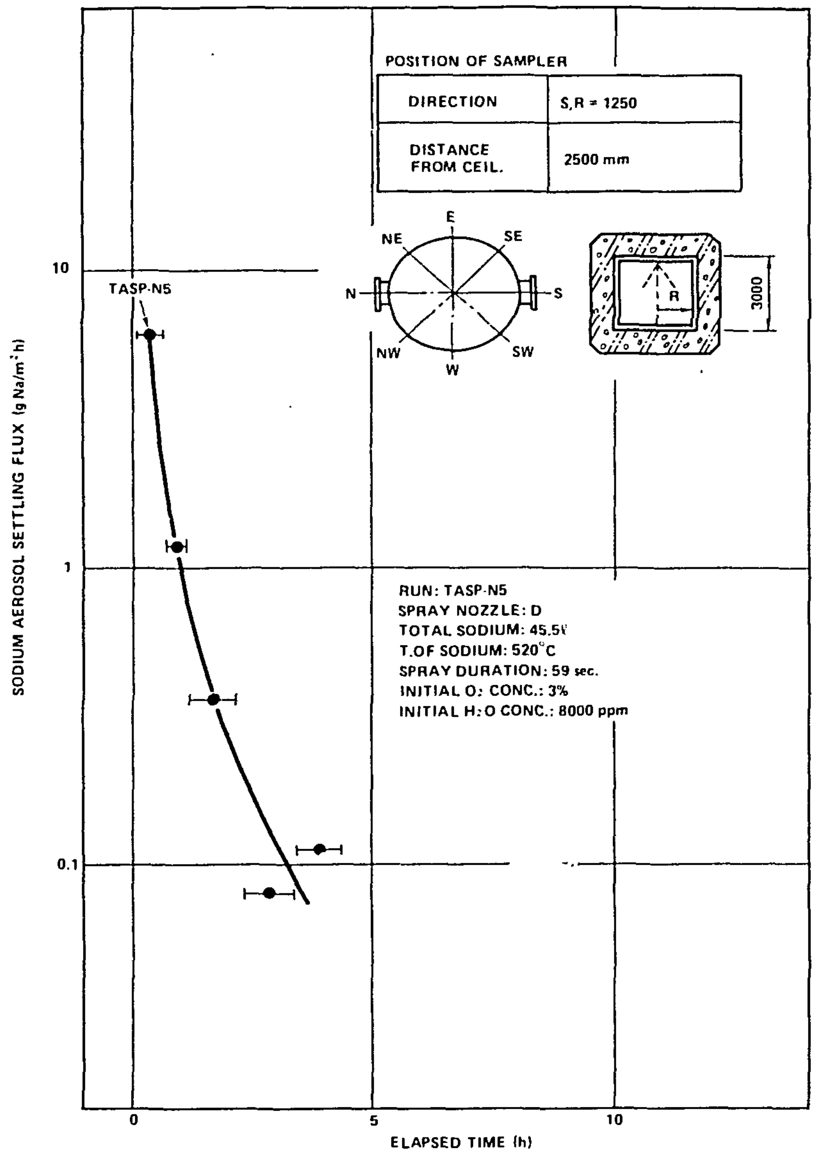

Fig. 4 Transistion of Aerosol Setting Flux after Spray Discharge in Nitrogen-filled Closed Space

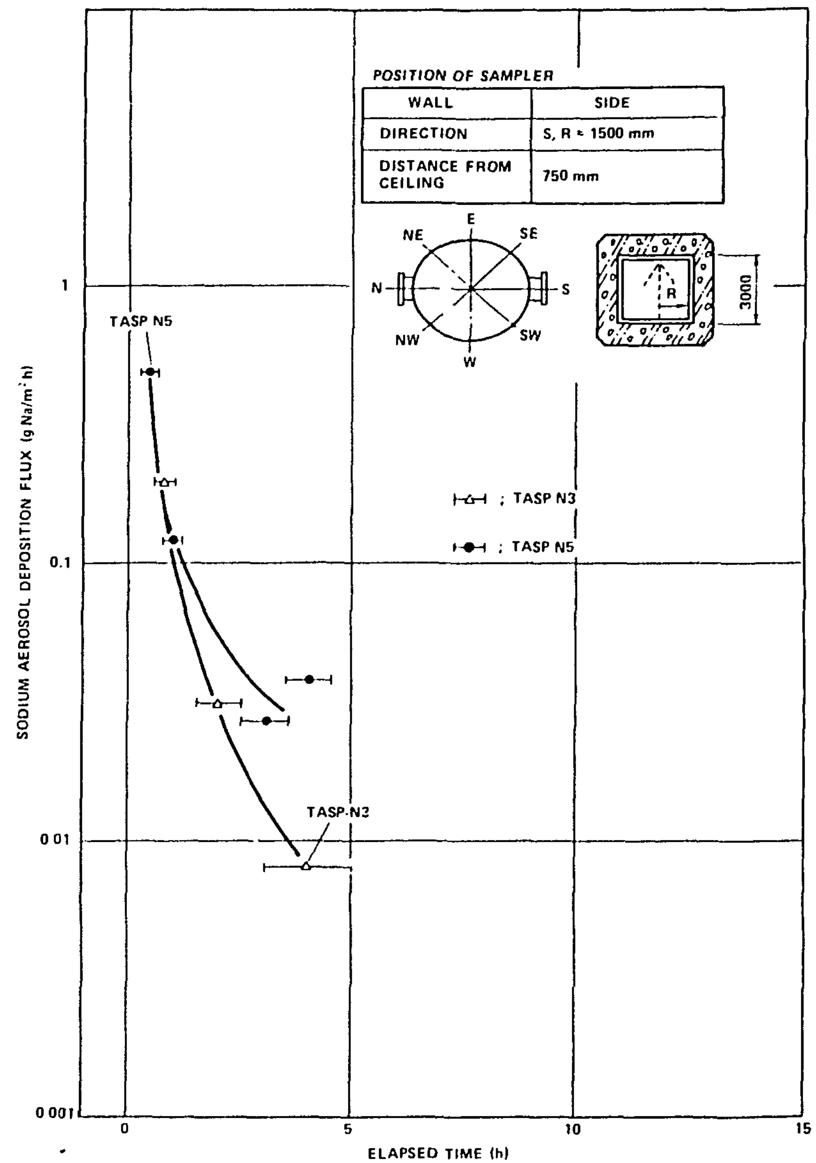

Fig. 5 Transition of Aerosol Deposition Flux to Side Wall after Spray Discharge in Nitrogen-filled Closed Space

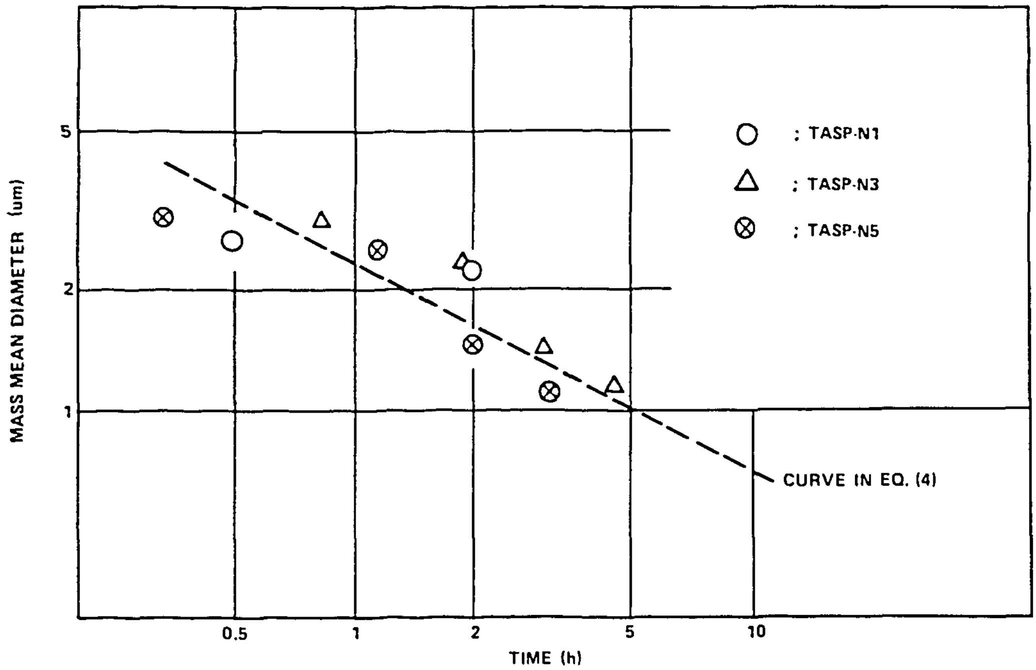

Fig. 6 Transition of Aerosol Mass Mean Diameter

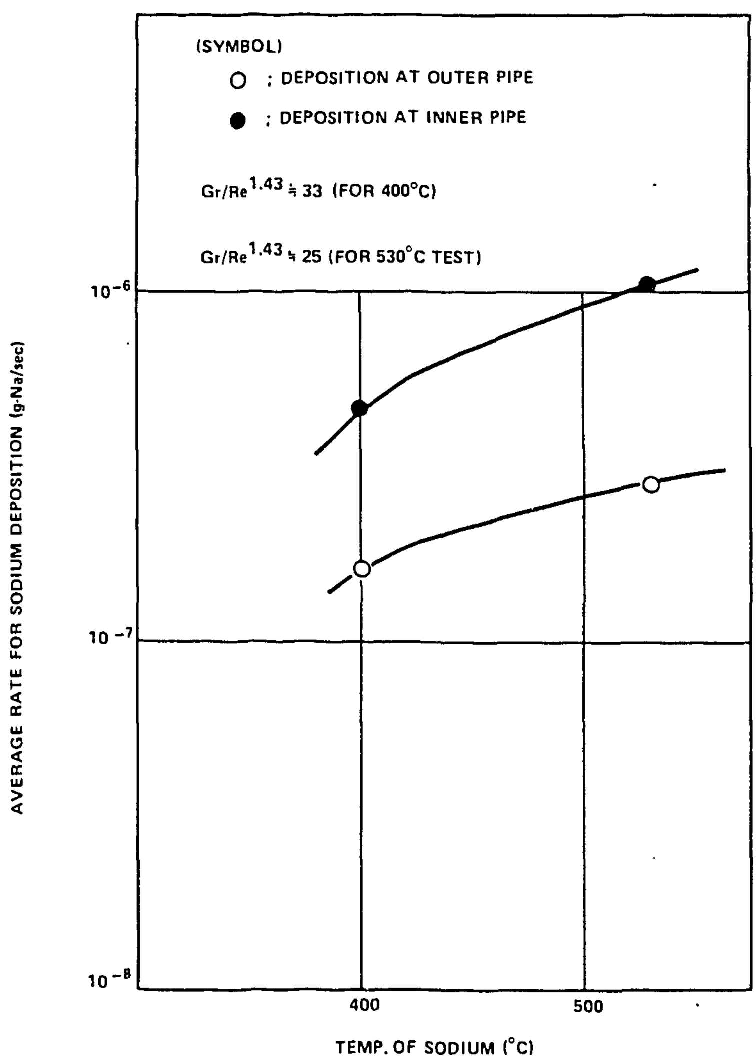

Fig. 7 Sodium Deposition at Inner Pipe and Outer Pipe

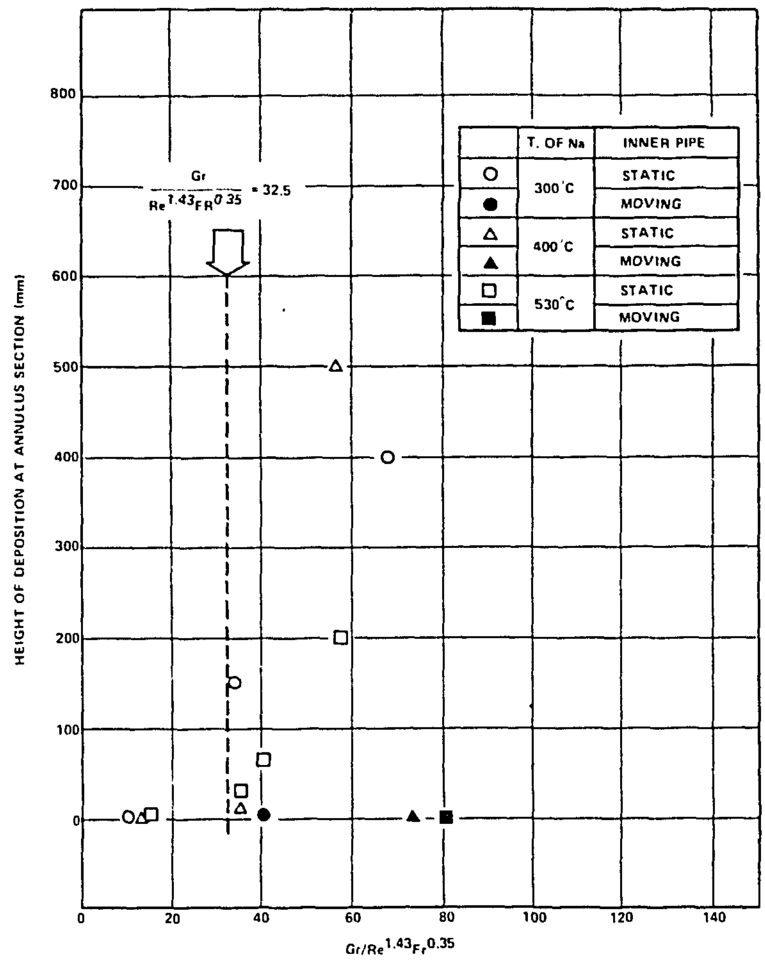

Fig. 8 Height of Deposition at Inner Pipe Versus $Gr/Re^{1.43}Fr^{0.35}$

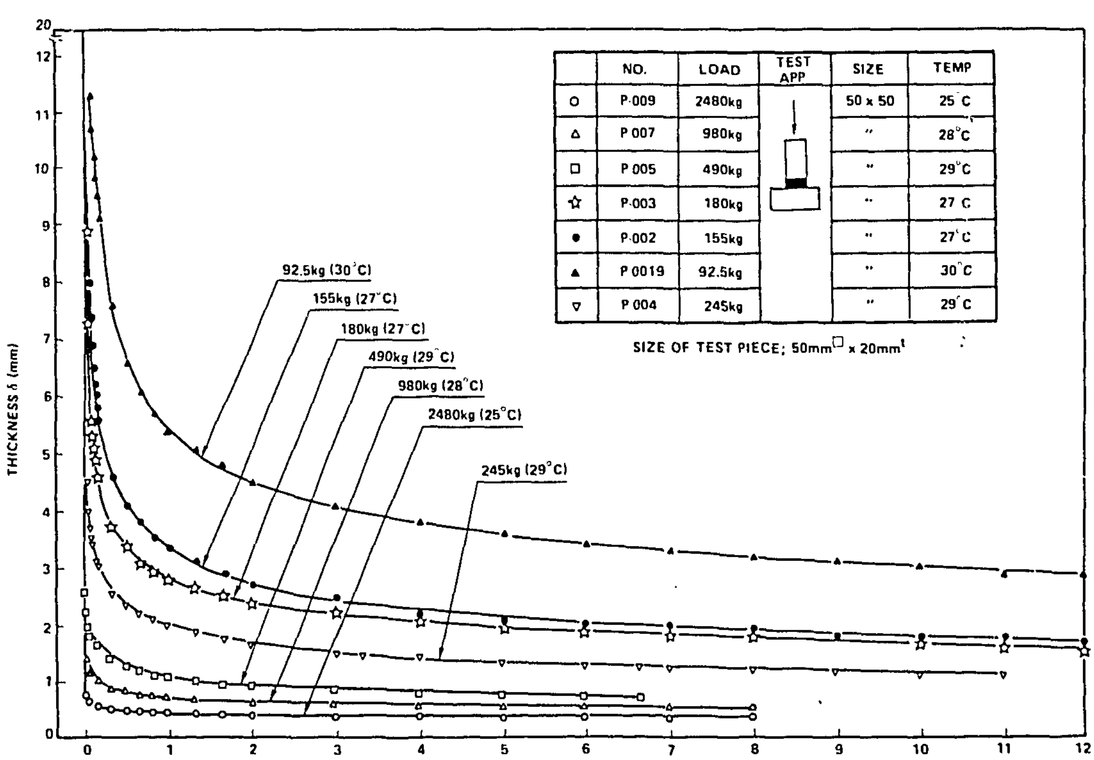

Fig. 9 Example of Compression Test for Solid Sodium; Thickness Versus Time